Interaction of Pipeline Materials with Molten Fluoride Salts

Oldřich Matal[a], Tomáš Šimo[a], Lukáš Nesvadba[a], Vladimír Dvořák[a], Viktor Kanický[b], Petr Sulovský[b], and Jiří Machát[b]

[a] ENERGOVÝZKUM, Ltd., Božetěchova 17, 612 00 Brno, Czech Republic
[b] Masaryk University, Faculty of Science, Kotlářská 2, 611 37 Brno, Czech Republic

Reprint requests to O. M.; E-mail: omatal@seznam.cz

Molten fluoride salts are very promising carriers for the transport of large amounts of heat for example from a high temperature nuclear reactor to a plant which generates hydrogen by chemical processes or from a nuclear reactor to a heat exchanger being a part of the equipment needed to realize the Brayton cycle with a very high power efficiency.

Therefore, in the framework of our project, experimental and theoretical investigations of the interactions of fluoride salts as heat carriers needed as high potential and structural materials for pipelines in order to transport heat at temperatures above 600 °C were started.

Experimental investigations of Fe-based and Ni-based materials in molten fluoride salts at high temperatures and with different exposure times were performed. Two components salts (LiF-NaF and NaF-NaBF$_4$) and three components salts (LiF-NaF-ZrF$_4$ and LiF-NaF-RbF) were chosen in the experiments. The salt analysis was focussed on the content of metallic elements before and after the exposure of the samples to the salt melts. It was done by inductively coupled plasma-optical emission spectrometry (ICP-OES) and by titrimetric techniques.

The thickness of the material zone affected by the salt melts, characterized by an enriched / reduced content of elements in comparison to the mean original content, and the material attacked zone, characterized by very tiny channels or chains of pores or pits formed preferably at grain boundaries, were the subject of the analysis performed by electron microscopy / microprobe techniques. Theoretical models for the transport of elements in the material samples exposed to salt melts using experimental data were also developed.

Key words: Fluoride Salts; Materials; High Temperature Interactions.

1. Introduction

To study interactions of pipeline structural materials and molten fluoride salts at temperatures above 600 °C experimental investigations of Fe-based and Ni-based materials at different exposure times in the framework of our project [1] have been performed. Experimental results and some comments about the interactions of the two components salt (numbers are mol%) 60LiF-40NaF and the three components salt 42LiF-29NaF-29ZrF$_4$ and 46.5LiF-6.5NaF-47RbF with stainless steel Nr. 1.4571 samples as a representative for a Fe-based material and with an alloy A686 sample as a representative for a Ni-based material at 680 °C under static or quasi-dynamic conditions are the main subject of this contribution.

2. Experimental

Each sample of the investigated material was put into the salt melt inside an ampoule made from the same material as the sample. Investigation was performed either in static or in quasi-dynamic conditions. Static conditions (called the first mode of experiments) mean that the sample does not move in the salt melt, while in quasi-dynamic conditions the sample moves periodically in the salt melt with a mean velocity of approximately 0.03 m/s (called the second mode of experiments).

During each of the experiments the temperature of the capsule and also the temperature of the salt melt inside the ampoule were controlled and held at the constant value.

After loading the salt and the samples of the investigated material into the ampoule, the capsule was connected with the experimental equipment which consisted of a vacuum system, argon cover gas and a heating furnace [2, 3].

Salt analyses before and after sample exposure to the salt melts were carried out by inductively coupled plasma-optical emission spectrometry (ICP-OES) and titrimetric techniques.

The cooled ampoule containing the solidified salt melt was cut into three parts. The salt was then mechanically sampled from identified zones and put into a ball mill. Powdered material was further processed for an ICP-OES solution analysis and a volumetric determination of fluorides.

The ICP optical emission spectrometer (JY-170 Ultrace, Jobin-Yvon, France) with lateral plasma observation was used for elemental analysis. The spectrometer was provided with both a mono- and a polychromator, which offer practical resolutions of 4 pm and 20 pm, respectively, for both systems (Czerny-Turner and Paschen-Runge mounts).

For the ICP-OES determination of the content of corrosion products in the exposed salt, 500 mg of powdered salt were dissolved after homogenization in 25 ml of aqua regia in a PFA beaker by heating. The obtained solution was diluted with de-ionized water to 500 ml in a volumetric flask and filtered (0.45 μm pore size) to remove insoluble residues. Determination of Li and Na by ICP-OES and F by titration was performed in aqueous leachates of the powdered solidified salt. Use of acids was avoided to prevent the solution from fluoride loss through volatilization of HF. Components of the nebulization and aerosol transport system made of PFA and Teflon® were used because of the aggressiveness of the fluorides to glass kits.

The limit of detection (LOD) used for the individual metals (the corrosion products) was 0.01%. Lower metal contents could not be measured. The precision defined as the uncertainty of the result was expressed for each sample as expanded (combined standard) uncertainty (coverage factor $k = 2$). Typical values of uncertainty for the alkali metals and the fluoride content were about 1% (relatively) and below (for the titrimetric determination of fluoride). For corrosion products, the uncertainty values from the ICP-OES measurements ranged between 2% and 20−30% (for elements with LOD levels).

The accuracy can be influenced by included matrix elements (mainly alkali metals). The effect of alkali metals on the results was eliminated using matrix-matched standards for the ICP-OES calibration.

Material samples before and after exposure to the salt melts were analyzed by electron microscopy/microprobe techniques.

The samples were embedded into epoxy resin (Araldite) disks and lapped and polished with diamond pastes to obtain sections for the study of concentration gradients over the alloy/adhered salt film interface. Such specimen were subjected to linear scanning, 2D elemental mapping and spot analyses in profiles perpendicular to the inner wall surface by electron probe microanalysis (EPMA).

The polished sections used for quantitative spot analyses, content profiles and elemental mapping were first covered with a 250 nm thick carbon layer to avoid charging at the alloy-salt (epoxy) interface.

Electron probe microanalysis was performed with an SX100 microprobe instrument (CAMECA, France), equipped with five crystal spectrometers, hosting six types of diffracting crystals (three layered pseudo-crystals for analysis of light elements, TAP, and large LIF and PET crystals). Images in secondary electrons (SE) were acquired to study the material morphology. Backscattered electron (BSE) images (material contrast) and cathode luminescence images were taken of polished cross-sections and relief specimen.

Quantitative spot analyses were run in profiles perpendicular to the ampoule wall; in the first $50−70\ \mu$m from the wall/melt interface the distance between individual spots was $2.5−5\ \mu$m, in the bulk between 50 and $250\ \mu$m the distance was $10−20\ \mu$m.

The acceleration voltage of 15 kV was chosen as a compromise between higher voltages used in metallurgy (20 − 25 kV) and lower voltages used in the analysis of volatile elements (10 kV). The analyzed spot size was $1\ \mu$m. The following analytical lines / standards were used: Fe K_α (pure Fe), Ni K_α (pure Ni), Co K_α (pure Co), Mn K_α (pure Mn), Cu K_α (pure Cu), Ti K_α (synthetic TiO_2), Si K_α (wollastonite), F K_α (synthetic LiF), Na K_α (jadeite), Mo L_α (pure Mo), W M_α (pure W), S K_α (pyrite). The standardization was checked for interferences and cross-checked with stainless steel standard SRM 460b (SPI). The acquired quantitative data were corrected using the modified ZAF method (PhiRoZet, CAMECA).

With the large-area crystals, the limits of determination can go down to tens of ppm, at common acquisition times, $2 − 3 \cdot 10^{-2}$% are usually achieved.

Sample	Mass concentration (%) of impurities determined in the salt (salt composition, mol%)		
	60LiF-40NaF	42LiF-29NaF-29ZrF$_4$	46.5LiF-6.5NaF-47RbF
Stainless steel 1.4571	0.60	0.351	0.175
Ni-based alloy A686	0.36	0.158	0.155

Table 1. Total mass concentration (mass%) of impurities in the salt after the exposure of material samples to the salt melt (680 °C, quasi-dynamic conditions).
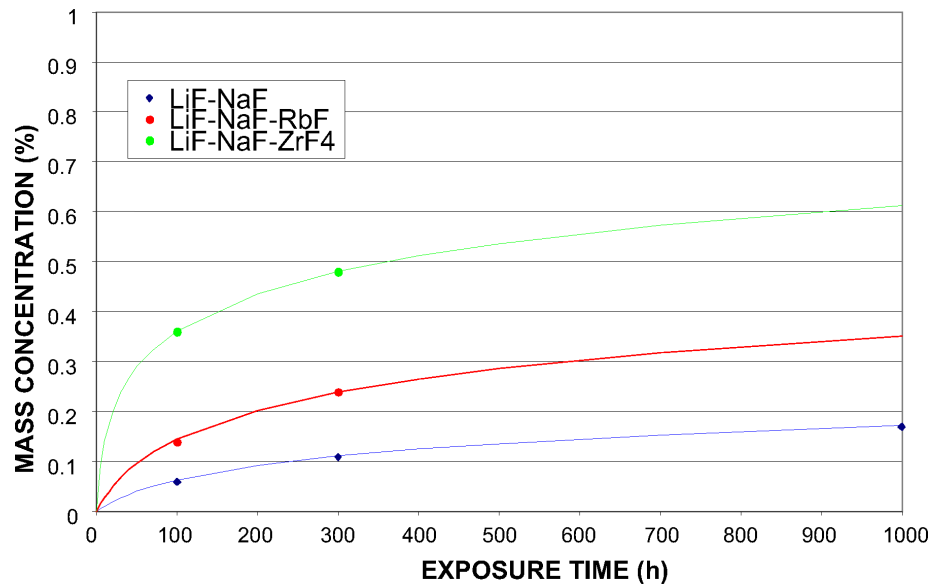

Fig. 1. Total mass concentration of impurities in the salt after the experiments versus the 1.4571 steel samples exposure time (680 °C, quasi-dynamic conditions).

3. Results

The total mass concentration (mass percentage) of impurities determined in the salt after the experiments for three salt compositions and two materials is given in Table 1.

The term "impurities" means the sum of metallic elements found in the salt, having its origin in the material of the sample. The elements Ni, Fe, Cr, Mo, Ti, Co, Mn and V have their origin in the stainless steel and W in the Ni-based alloy.

The temporal kinetics of the total mass concentration of impurities in the salt after the experiments at 680 °C follows from Figure 1.

The thickness of the material affected zone (or affected depth from the sample surface) by the salt melt after 1000 h of exposure at 680 °C is presented in Table 2. The affected zone is the zone influenced by the salt melt and characterized by an enriched content of some elements (for ampoule Ni and Mo) or/and reduced content of some elements (for example Cr) in comparison to the mean original element content in the material of the sample.
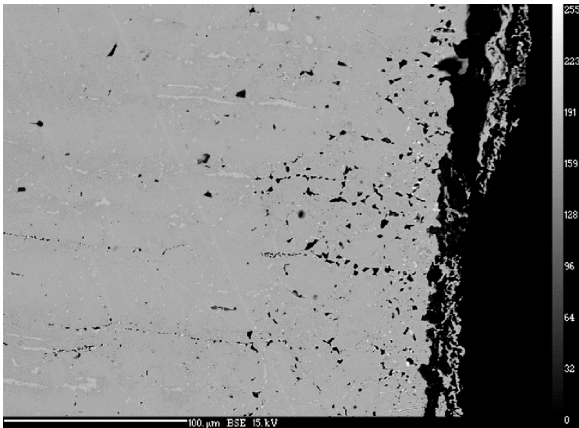

Fig. 2. Stainless steel sample, cross-section after exposure (680 °C, 1000 h, LiF-NaF-RbF salt, quasi-dynamic test conditions).

The character of the attacked zone is very different, depending on the material of the sample and the salt melt composition. Very tiny channels or chains of pores or pits formed preferably at grain boundaries have been observed in this zone. For example in Fig. 2

Sample	Affected depth (μm) from the sample surface determined after the experiments in the salt melt		
	60LiF-40NaF	42LiF-29NaF-29ZrF$_4$	46.5LiF-6.5NaF-47RbF
Stainless steel 1.4571	24 – 29	25 – 30	> 25
Ni-based alloy A686	26 – 30	22 – 24	11 – 12

Table 2. Thickness of the affected zone by salt melts after 1000 h of exposure (quasi-dynamic regime) characterized by enriched / depleted content of elements in comparison to the mean original content.
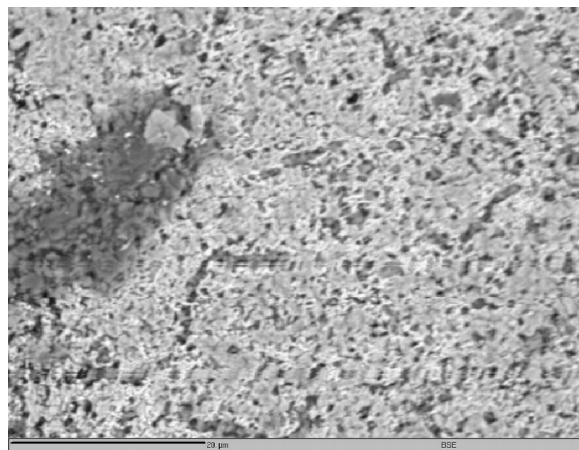

Fig. 3. Alloy A686 sample, view at the surface after exposure (680 °C, 1000 h, LiF-NaF-RbF salt, quasi-dynamic test conditions).
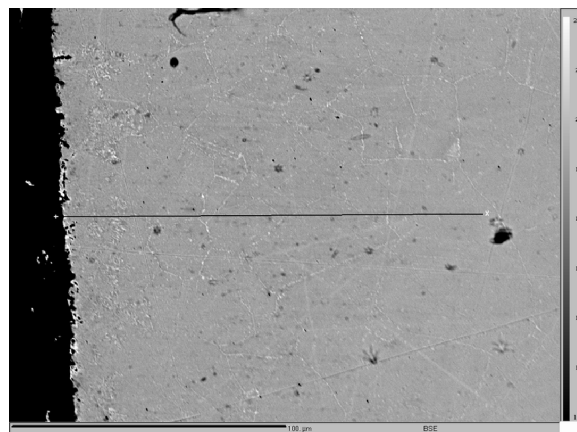

Fig. 4. Alloy A686 sample, cross-section after exposure (680 °C, 1000 h, LiF-NaF-RbF salt, quasi-dynamic test conditions).

a cross-section of the steel sample with an intensive intergradual attack, in Fig. 3 a view on the surface of the A686 alloy sample after exposure, and in Fig. 4 a cross-section of the A686 sample with a very fine pitting corrosion in the surface layer both after 1000 h exposure to the LiF-NaF-RbF salt melt is shown.

The influence of static and quasi-dynamic conditions at 680 °C on the corrosion rate of both materials in the 60LiF-40NaF melt is demonstrated in Figure 5.

4. Corrosion and Mass Transfer Model

A number of models of corrosion and mass transfer can be found in the literature. The model published in [4] for corrosion and mass transfer of steels in sodium, based on the solution of the diffusion equation with the error function, was modified and applied for steels in molten fluoride salts in [5].

The model requires many important parameters which can be determined only from experimental data analysis. But in case of salt impact studies it has been almost impossible to determine input parameters directly from measured data. It was necessary to use some additional methods.

One of the most important input parameters for the model is the surface concentration of the studied element. It was very difficult to determine this parameter, because the steel sample surface was largely disintegrated by salt impact, and it was a problem to locate the sample surface exactly. It was necessary to analyze many measurements and to determine common features of the shapes of the element distribution curves. On the basis of this analysis the location of the sample surface was determined and of course also the surface element concentration.

The second significant problem was to determine the velocity of the sample surface caused by the mass transfer of elements to the salt or to the centre of the sample because of the fact that the whole surface of the sample was immersed in the salt solution (not only the measured part of the surface). This velocity was determined by weighing the sample after exposure and also by measuring of the element concentration in the salt. These two values were compared and the value of the velocity was determined from the ratio of the measured surface to the whole surface.

The third parameter, determined by additional analysis, is the so-called resistivity factor. One of the possible ways to determine this factor is to fix the tangent of the element distribution at the point of the sample surface. In order to do this, the first problem was to determine the sample surface as is described
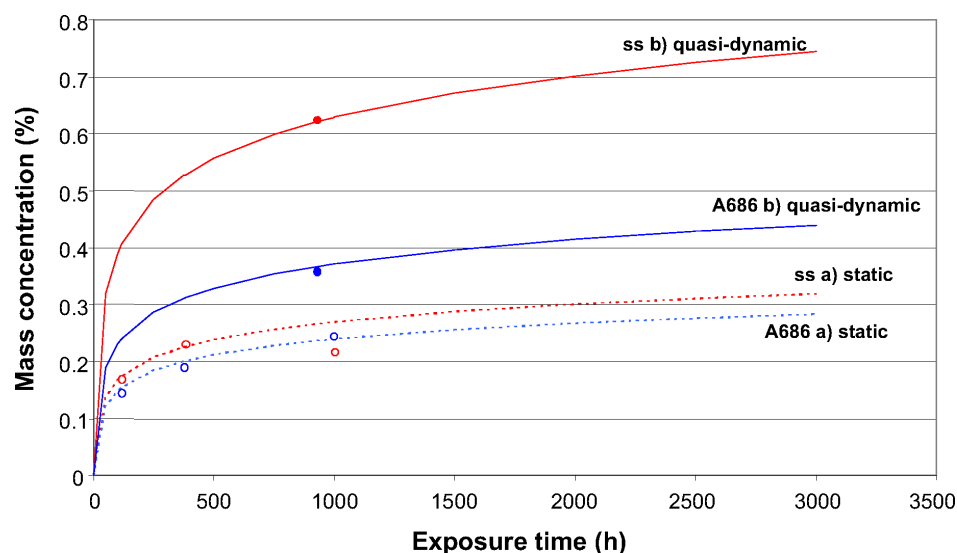
Fig. 5. Comparison of the mass concentration of impurities in the 60LiF-40NaF (mol%) salt melt after the exposure of stainless steel (ss) and A686 alloy (A686) samples in static and quasi-dynamic conditions.
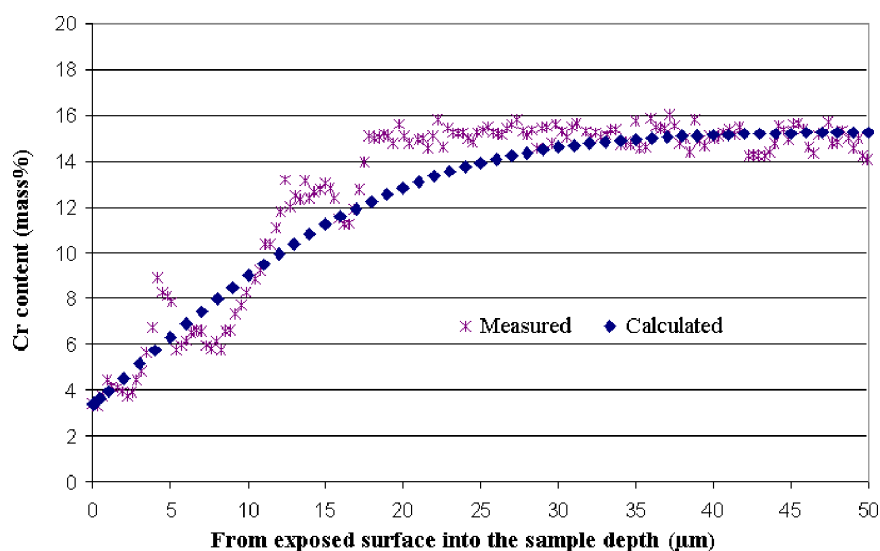

Fig. 6. Calculated and measured chromium distribution in the sample made from austenitic steel 1.4571 after 930 h of exposure to the 60LiF-40NaF (mol%) salt at 680 °C (quasi-dynamic conditions).

above. The second problem was to construct a tangent to the curve shown in Figure 6. After some tests it was decided to replace the tangent by a straight line obtained from linear regression of the whole increasing part of the distribution curve. So the regression line in fact is not the tangent but the secant.

On the basis of the above mentioned considerations and the additional analysis the necessary input parameters for the model were obtained and the element distribution in the measured sample was then calculated.

The calculated and the directly measured chromium distribution in the steel 1.4571 sample exposed 930 h to the salt melt consisting of 60LiF-40NaF (mol%) at 680 °C is shown in Figure 6.

From Fig. 6 it can be seen that the chosen diffusion model describes the experimental data well. Thus one can conclude that one of the possible corrosion processes at the salt-steel interface could be diffusion. But it is rather difficult to assess the rate of the diffusion process in comparison with other corrosion mechanisms, because the significant input data for the model

were obtained by indirect methods from the experiment.

5. Conclusion

Selected results found by exposure of two samples, stainless steel Nr. 1.4571 and Ni-based alloy A686, in three fluoride salt melts (60LiF-40NaF; 42LiF-29NaF-29ZrF$_4$; 46.5LiF-6.5NaF-47RbF; all numbers are mol%) at 680 °C have been reported. These results demonstrate that:

- Ni-based materials are more resistive to fluoride salt melts in comparison to Fe-based materials;
- very different effects of fluoride salts with different composition to one structural Ni-based alloy (for example A686) at the same conditions can be expected for high temperature applications (see Fig. 1 and Table 2).

[1] O. Matal, Project Nr. 101/04/0872, Grant Agency of the Czech Republic.
[2] O. Matal, T. Šimo, L. Nesvadba, V. Kanický, P. Sulovský, and J. Machát, Some results of corrosion tests of materials in fluoride molten salts, in: Proceedings of the 7th International Symposium on Molten Salts Chemistry and Technology, 29.8. – 2.9.2005, Toulouse, France.
[3] L. Nesvadba, T. Šimo, O. Matal, and M. Vávra, Equipments and methods for studies of salt melts influence on structural materials, in: Proceedings of the 5th Nicholas's Young Generation Informal Meeting, 13. – 15.12.2005, Brno, Czech Republic.
[4] T. Yonezawa, T. Saida, Y. Watanabe, and T. Kiyokawa, Computer analysis of the corrosion and mass transfer of steels in sodium, in: Proceedings of the 3rd International Conference on Liquid Metal Engineering and Technology, 9. – 13. April 1984, Oxford, UK.
[5] V. Dvořák and O. Matal, Design, Software and Application of a Diffusion Model of Steel – Fluoride Salt Melt Interactions, Report QR-EM-043-05, Energovyzkum, Ltd., Brno 2005.